Density-functional studies of magnetic and electronic structures for the perovskite oxides $LaMn_{1-x}Cr_xO_3$

2000 J. Phys.: Condens. Matter 12 2737

(http://iopscience.iop.org/0953-8984/12/12/313)

J. Phys.: Condens. Matter **12** (2000) 2737–2747. Printed in the UK PII: S0953-8984(00)09691-0

Density-functional studies of magnetic and electronic structures for the perovskite oxides $LaMn_{1-x}Cr_xO_3$

Zhongqin Yang, Ling Ye and Xide Xie

Surface Physics Laboratory (National Key Laboratory), Fudan University, Shanghai, 200433, China

Received 18 November 1999

Abstract. The magnetic and electronic properties of the Mn-site-doped perovskite oxides $LaMn_{1-x}Cr_xO_3$ ($x = 0.0, 0.25, 0.5, 0.75, 1.0$) are studied theoretically by using the tight-binding linear muffin-tin orbital method. Rather than ferromagnetic structures, ferrimagnetic ones of a certain type are found to be the most stable states for compounds with intermediate doping levels; this is related to the strong positive Mn^{3+}–Mn^{3+} interaction and negative Cr^{3+}–Cr^{3+} interaction. The reasons for there being these two kinds of interaction are analysed. The total magnetic moments for the doped compounds increase with x varying from 0.0 to about 0.25; this is in good agreement with experimental results. For the doped compounds with $x = 0.5$ and 0.75, in addition to the distorted orthorhombic structures, the cubic structure has also been studied. In addition to being found for the doped compound with $x = 0.5$ (with interlacing-type doping), half-metallic bands have also been found for the doped compound with $x = 0.75$ both with ferromagnetic and ferrimagnetic (in several types) interaction.

1. introduction

Because of their rare properties, such as the 'colossal' magnetoresistance (CMR) observed near room temperature [1, 2], and the temperature-dependent structural phase transition induced by an external magnetic field [3], the La-site-doped perovskite oxides $La_{1-x}D_xMnO_3$ with D = Ca, Sr, Ba have attracted considerable attention for the past few years [4–6]. Recently, people have begun to investigate properties of Mn-site-doped systems, such as $LaMn_{1-x}Co_xO_3$ [7, 8], in order to investigate their CMR property. The Mn-site-doped compounds, such as $LaMn_{1-x}Cr_xO_3$, are also very important because of their solid-oxide fuel cell applications [9]. Although the electronic states of those Mn-site-doped perovskites (including $LaMn_{1-x}M_xO_3$ (M = Cr, Fe, Co, Ni, Ga)) have been studied widely [10–12], there are still controversies as regards the results obtained by various authors.

For example, ferromagnetic (FM) structure has been suggested by Gilleo [13] for $LaMn_{1-x}Cr_xO_3$, while the conclusions of Jonker [14] and Bents [12] were different. Jonker [14] obtained the saturation magnetization of the system, which reaches its maximum value at the point of the structural transition from monoclinic to cubic structure ($x = 0.3$). Strong positive Mn^{3+}–Mn^{3+} and Mn^{3+}–Cr^{3+} interactions and a negative Cr^{3+}–Cr^{3+} one were suggested by Jonker [14] to explain the decrease in total magnetization in the cubic structure with x varying from 0.3 to 1.0. Bents [12] studied the magnetic structures of the compounds by using neutron diffraction. Also in contrast to the suggestion of Gilleo [13], Bents found that in addition to FM structure, A-type antiferromagnetic (A-AFM) and G-type antiferromagnetic (G-AFM) structure also exist in compounds with very small Cr concentrations ($x < 0.15$) and large

0953-8984/00/122737+11$30.00

Cr concentrations ($x > 0.3$), respectively. Thus, it is obvious that there exist discrepancies among these descriptions for the properties of the doped compounds. In order to resolve some of the controversies and to provide some help in understanding the CMR mechanism, it is important to study systematically the electronic and magnetic properties of the Mn-site-doped compounds.

In the present work, a systematic theoretical investigation of the properties of $LaMn_{1-x}Cr_xO_3$ ($x = 0.0, 0.25, 0.5, 0.75, 1.0$) has been performed. For compounds with intermediate doping levels, it has been found that ferrimagnetic (FiM) structures of certain types are more stable than the FM states. From the spin directions of Mn 3d and Cr 3d states in the unit cells, it can be concluded that it is FM Mn^{3+}–Mn^{3+} interactions and AFM Cr^{3+}–Cr^{3+} ones which cause the total moments to increase first and then decrease when x varies from 0.0 to 1.0. The reasons for there being FM interaction between two Mn ions and AFM interaction between Cr ions have been analysed. Half-metallic bands, which are believed to be related to the CMR properties, have been found for the doped compound with $x = 0.75$ (hereafter referred to as the '0.75-doped compound') with various magnetic structures and the FM 0.5-doped compound with interlacing-type doping, which will be described later.

2. Crystal structures and method

The experimentally observed crystal structures of $LaMn_{1-x}Cr_xO_3$ [12, 13] have been used in the calculation with the orthorhombic *Pnma* unit cell (the monoclinic structures reported in reference [12] could actually be transformed into orthorhombic ones). The lattice constants at special doping levels ($x = 0.25, 0.5, 0.75$) are obtained by linearly interpolating between the experimental points. Table 1 gives the lattice parameters (in Å) used for $LaMn_{1-x}Cr_xO_3$ ($x = 0.0, 0.25, 0.5, 0.75, 1.0$). Table 1 also lists the volumes (in $Å^3$) per unit cell and the proportions of the three lattice constants, from which the strength of the distortion from cubic structure can be evaluated. The volumes shown in table 1 decrease with the increase of the level of Cr doping. For cubic structures, the ratio of the coefficients $a{:}b{:}c/\sqrt{2}$ is equal to 1:1:1. From comparing the coefficients of the compounds listed in table 1, it is known that the crystal distortions in the 0.25-, 0.5- and 0.75-doped compounds are all smaller than that of $LaMnO_3$, and that the structures of these compounds are close to the cubic structure (especially for the 0.25-doped compound). From table 1, it can be seen that the distortion in $LaCrO_3$ is also smaller than that in $LaMnO_3$. Three different doping types have been considered for the 0.5-doped compound. Since the ideal cubic structures have been reported by Jonker [14] for compounds with the doping level $x \geqslant 0.3$, the ideal cubic structures, which have the same volumes per unit cell as the corresponding orthorhombic structures, have been considered in the calculation for the 0.5- and 0.75-doped compounds. The electronic and magnetic properties of the compounds have been studied by using the tight-binding linear

Table 1. Lattice parameters (in Å) used for $LaMn_{1-x}Cr_xO_3$ ($x = 0.0, 0.25, 0.5, 0.75, 1.0$). The volumes (in $Å^3$) per unit cell and the proportions of the lattice parameters are also listed.

	a	b	c	Volume	$a{:}b{:}c/\sqrt{2}$
$LaMnO_3$	5.533	5.744	7.693	244.496	1.017:1.056:1
$LaMn_{0.75}Cr_{0.25}O_3$	5.513	5.517	7.814	237.666	1:1.001:1.002
$LaMn_{0.50}Cr_{0.50}O_3$	5.492	5.520	7.780	235.857	1:1.005:1.002
$LaMn_{0.25}Cr_{0.75}O_3$	5.488	5.513	7.761	234.812	1:1.005:1.000
$LaCrO_3$	5.481	5.518	7.735	233.939	1.002:1.009:1

muffin-tin orbital atomic-sphere approximation (the TB-LMTO-ASA) method [15] based on the local spin-density approximation (LSDA). Since the method is only suitable for close-packed structures, empty spheres have been inserted appropriately in the interstitial regions of the unit cells. In the calculation, La 6s, 5d and 4f, Mn (Cr) 4s, 4p and 3d and O 2p orbitals have been considered as the valence states. It is known that the La 4f and 5d states lie about 4–5.5 eV and 3–8 eV above the Fermi level (E_F), respectively; these states together with the weak-intensity La 6s, Mn (Cr) 4s states have no obvious effects on the results, and therefore are not analysed in detail in the following.

3. Results and discussion

3.1. Two end-members

The two end-members $LaMnO_3$ and $LaCrO_3$ are studied first, with A-AFM and G-AFM structure [16], respectively. Metallic and insulator bands have been obtained in the calculations for $LaMnO_3$ and $LaCrO_3$, respectively, while in experiments, insulating bands have been found for both compounds [17]. The discrepancies between the theoretical and experimental results for the two end-members are mainly related to the underestimated correlation interaction between electrons in the LSDA and can be reduced by considering the Hubbard-like interaction term in the standard LSDA, i.e. using the LSDA + U method [18]. The local magnetic moments of Cr ions in $LaCrO_3$ and Mn ions in $LaMnO_3$ are about 2.65 and 3.43 μ_B, respectively; they are comparable with the experimental results, 2.8 ± 0.2 μ_B [19] and 3.7 ± 0.1 μ_B [20], respectively. The valence bandwidths of the two compounds are both about 7.0 eV, and the occupied 3d states of Mn and Cr ions are located at higher energy and closer to the Fermi level (E_F) than the O 2p states. Figures 1(a) and 1(b) give the partial densities of states (DOS) for the transition-metal-ion (Mn, Cr) 3d states and for the O 2p states, for A-AFM $LaMnO_3$ and

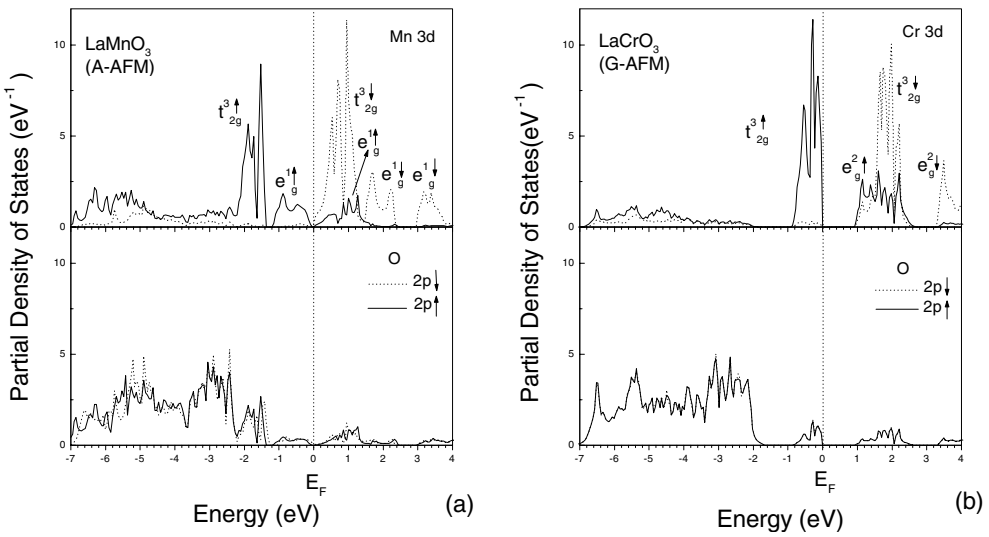

Figure 1. (a) The partial Mn 3d and O 2p densities of states in $LaMnO_3$ with the observed A-AFM state. (b) The partial Cr 3d and O 2p densities of states in G-AFM $LaCrO_3$. The solid and dotted lines in the figures indicate spin-up and spin-down bands, respectively, and the vertical dotted line at the zero point gives the Fermi energy.

G-AFM $LaCrO_3$, respectively. The solid and dotted lines in the figures indicate the spin-up and spin-down bands, respectively. And the vertical dotted lines at the zero point give the positions of the Fermi energy, E_F. From figures 1(a) and 1(b), it is known that the exchange splittings between the spin-up and corresponding spin-down bands of the transition-metal ions (Mn and Cr) are large (about 2.5 and 2.0 eV for $LaMnO_3$ and $LaCrO_3$, respectively). Although both $LaMnO_3$ and $LaCrO_3$ were studied with antiferromagnetic structures, there is more obvious spin polarization in the O 2p states in $LaMnO_3$ than in $LaCrO_3$, which is due to the distortion from cubic structure in $LaMnO_3$ being larger than that in $LaCrO_3$ [12] (see table 1); thus the two sets of spin-up and spin-down sublattices in $LaMnO_3$ are more different than those in $LaCrO_3$.

3.2. Magnetic structures

Ferromagnetic structures have been studied for the doped compounds with intermediate levels of Cr doping together with the two end-members. The total magnetic moments shown in figure 2 by the 'diamond' symbols on the dotted line decrease linearly from 3.9 to 3.0 μ_B with the doping level varying from 0.0 to 1.0. By comparing with experimental results obtained by Jonker [14] (shown by plus signs (+)), it can be seen that the total moments obtained are much larger—by at least 1.7 μ_B. Therefore, compounds with FM structure cannot be in the ground state. Since it is known that A-AFM and G-AFM structures are the most stable states for $LaMnO_3$ and $LaCrO_3$, respectively, several different kinds of magnetic structure have been considered for compounds with intermediate doping levels in order to find the most stable one. Due to the complexity of the calculation, only the primitive unit cells [5], which contain 20 atoms (four La, four Mn (Cr), twelve O), have been used to study the magnetic properties for those compounds. All five magnetic structures have been considered for 0.25- and 0.75-doped compounds and six for the 0.5-doped compound; these are all listed in table 2. The four spin directions in each magnetic structure in table 2 correspond to the spin directions of the four non-equivalent transition-metal ions (Mn^{3+} or Cr^{3+}) in the unit cell, which are labelled as I, II,

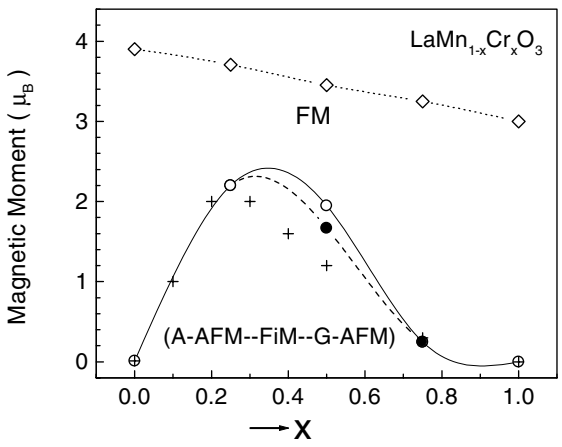

Figure 2. The total magnetic moment in $LaMn_{1-x}Cr_xO_3$ varying with the doping level x. The 'diamond' symbols on the dotted line represent the moments for the FM phase. The open circles on the solid line represent the results obtained with the distorted structures in the present calculation; the two solid dots on the dashed line represent our calculated results obtained with cubic structures; the plus signs (+) represent the experimental results of Jonker [14]. The results obtained with distorted and cubic structures for the 0.75-doped compound are just the same.

Table 2. Calculated relative energies (in meV/unit cell) of various magnetic structures of $LaMn_{1-x}Cr_xO_3$. The energies of the FM phase are used as the reference energy for compounds with different Cr doping levels. The total magnetic moments (μ_B/unit cell) in each case are also listed. Subscripts 'm', 'c' represent Mn and Cr ions, respectively.

$LaMn_{0.75}Cr_{0.25}O_3$						
Magnetic structure	$\uparrow_m\uparrow_m$ $\uparrow_m\downarrow_c$	$\uparrow_m\uparrow_m$ $\uparrow_m\uparrow_c$	$\uparrow_m\uparrow_m$ $\downarrow_m\downarrow_c$	$\uparrow_m\downarrow_m$ $\uparrow_m\downarrow_c$	$\uparrow_m\uparrow_m$ $\downarrow_m\uparrow_c$	
Relative energy	−31.3	0.0	136.0	170.0	197.2	
Magnetic moment	8.816	14.826	0.639	0.725	6.911	
$LaMn_{0.50}Cr_{0.50}O_3$						
Magnetic structure	$\uparrow_m\uparrow_m$ $\uparrow_c\downarrow_c$	$\uparrow_m\uparrow_m$ $\downarrow_c\downarrow_c$	$\uparrow_m\uparrow_m$ $\uparrow_c\uparrow_c$	$\uparrow_m\downarrow_m$ $\downarrow_c\uparrow_c$	$\uparrow_m\downarrow_m$ $\uparrow_c\downarrow_c$	$\uparrow_m\downarrow_m$ $\uparrow_c\uparrow_c$
Relative energy	−93.8	−80.2	0.0	136.0	178.2	193.1
Magnetic moment	7.784	1.763	13.806	0.025	0.031	6.028
$LaMn_{0.25}Cr_{0.75}O_3$						
Magnetic structure	$\uparrow_m\downarrow_c$ $\downarrow_c\uparrow_c$	$\uparrow_m\uparrow_c$ $\downarrow_c\downarrow_c$	$\uparrow_m\downarrow_c$ $\uparrow_c\downarrow_c$	$\uparrow_m\downarrow_c$ $\downarrow_c\downarrow_c$	$\uparrow_m\uparrow_c$ $\uparrow_c\uparrow_c$	
Relative energy	−221.7	−198.6	−31.3	−6.8	0.0	
Magnetic moment	1.000	1.000	1.000	5.000	13.000	

III, IV ions in figure 3. For each compound with a different doping level, the energy of the FM phase serves as the reference energy for the relative energies shown in table 2. The magnetic structures for each compound are arranged in order, from that with lowest relative energy to that with the highest. Thus, the structures in the first column are the most stable ones among all the structures listed in table 2. Figures 3(a), 3(b) and 3(c) show the most stable magnetic structure in the unit cell for the 0.25-, 0.5- and 0.75-doped compounds, respectively (they are only sketch maps, and the non-magnetic La and O ions are not shown). From table 2, it is

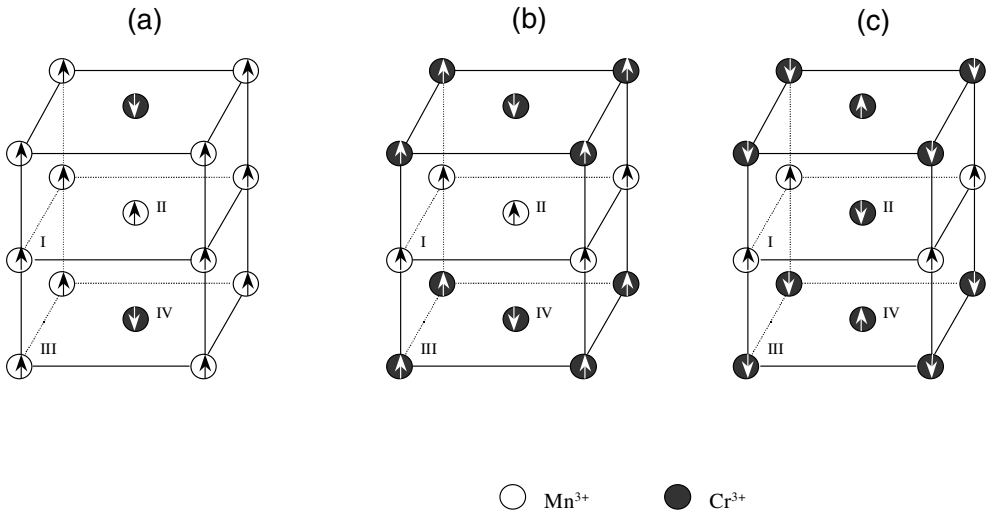

Figure 3. The calculated most stable magnetic structures in one unit cell for the doped compound, with levels of Cr doping of $x = 0.25$ (a), 0.5 (b) and 0.75 (c), respectively. Only the transition-metal ions Mn and Cr are shown. The ions labelled as I, II, III and IV are the non-equivalent atoms in the unit cell.

found that there exists at least one type of FiM structure which is more stable than the FM states for compounds with intermediate doping levels.

For the 0.25-doped compound, there are three Mn ions (labelled as I, II and III in figure 3(a)) and one Cr ion (labelled as IV in figure 3(a)) in the unit cell. From table 2, it can be seen that all states with the three Mn ions not in the same spin direction have larger relative energies than the FM states, by more than 136 meV per unit cell. Although the FM state has lower relative energy than the states mentioned above, it has higher relative energy than the state with the first magnetic structure shown in table 2 for the 0.25-doped compound. This means that the three Mn ions in the unit cell of the 0.25-doped compound tend to be in the FM state, while the Cr ion has the spin direction opposite to that of the Mn ions. It is known that $LaMnO_3$ is experimentally observed to have A-AFM structure [16] with FM ordering in the a–c plane, and AFM ordering between the a–c planes, while cubic $LaMnO_3$ is found to have a FM state (strong positive interaction between Mn^{3+} and Mn^{3+} ions) [5, 14]. Since the 0.25-Cr-doped compound has less distorted structure (a:b:$c/\sqrt{2}$ = 1:1.001:1.002), the structure of the compound can be dealt with approximately as a cubic one. Therefore, it is reasonable that the three Mn ions in the compound have FM interaction. Due to the e_g orbitals of Mn ions crossing E_F, metallic bands have been found for the 0.25-doped compound with the most stable FiM magnetic structure.

Three doping types have been studied for the 0.5-doped compound with the FM phase: the layer-by-layer type (two Mn (Cr) on the a–b plane); the interlacing type in which each Mn (Cr) atom is surrounded by six nearest Cr (Mn) neighbours; and the type with two Mn (Cr) aligning along the longest axes (in the c-direction). The third type is found to be unstable; the first one (layer by layer) is the most stable state with metallic bands; and half-metallic nature (with metallic spin-up bands and insulating spin-down bands), accompanied by an integral total magnetic moment per unit cell, is obtained for the interlacing doping type. The different magnetic structures have only been considered for the layer-by-layer doping type in the compound. In figure 3(b), one layer plane is contributed by Mn ions (labelled as I, II) and the other by Cr ions (labelled as III, IV). From table 2, it can be seen that all magnetic structures with AFM interaction between Mn ions have higher relative energies than that of the FM phase, while those structures with FM interaction between Mn ions have lower energies, which is the same as the case for the 0.25-doped compound. For the interaction between Cr ions, the compound with AFM Cr ions has lower relative energy than that with FM interaction. Thus, it can be concluded that the structure with FM interaction between Mn ions and AFM interaction between Cr ions is the most stable structure for the 0.5-doped compound with the layer-by-layer doping type. The FM interaction between Mn ions in the 0.5-doped compound occurs because the Mn–O–Mn bond lengths in the a–b plane are all nearly equal, which is similar to the case for Mn ions in the 0.25-doped compound.

For the 0.75-doped compound, the FM state is found to have the highest relative energy, compared to the other magnetic structures for the compound in table 2. Since in the 0.75-doped compound there are more Cr ions, and the interaction between Cr ions in both distorted [16] and cubic [14] structures is usually negative, the magnetic structure with AFM interaction between Cr ions must be more stable than that with FM interaction. In table 2, for the 0.75-doped compound, the fourth structure with FM interaction between Cr ions and AFM interaction between Mn and Cr ions has relative energy a little bit lower (−6.8 eV) than that of the last FM structure, while the first two structures on the left-hand side of the table with AFM Cr ions between two planes have much lower energies. It is understandable that the first magnetic structure with nearest-neighbour Cr ions having opposite spin orientations is the most stable for the 0.75-doped compound. The arrangement of the spin directions in the 0.75-doped compound is very similar to that of the end-member G-AFM $LaCrO_3$; by replacing the Mn

ion by Cr with the same spin orientation in the unit cell in figure 3(c), the magnetic structure of $LaCrO_3$ can be obtained.

From the above discussion, it can be concluded that the magnetic interactions between Mn^{3+} and Mn^{3+} ions and between Cr^{3+} and Cr^{3+} ions in the doped compound $LaMn_{1-x}Cr_xO_3$ are ferromagnetic and antiferromagnetic, respectively. Due to the small distortion in the compounds with the intermediate doping levels, the conclusion reached on the basis of the calculation can be compared to the results obtained by Jonker [14], who found cubic structure for a compound with $x \geqslant 0.3$ and positive and negative magnetic interaction energies for Mn^{3+} and Mn^{3+} ions and Cr^{3+} and Cr^{3+} ions, respectively, for the cubic perovskites. This conclusion is also reached from our calculation. Positive interaction energy was, however, also obtained by Jonker [14] between Mn^{3+} and Cr^{3+}, which is not found in the present calculation. In table 2 the total magnetic moments per unit cell corresponding to each magnetic structure are also listed. It is found that the moments for FM structures are much larger than those of FiM structures for each doped compound, and the FM moment decreases almost linearly with the increase of the level of Cr doping. The moments (μ_B per formula unit (/Mn)) of the most stable magnetic structure in table 2 for each doped compound also decrease with the variation of the doping level x from about 0.3 to 0.75, which is represented in figure 2 by open circles on a solid line. The plus signs '+' in figure 2 represent the experimental saturation magnetizations obtained by Jonker [14]. Comparing the two sets of results, it is found that except for the compounds with x at 0.5, the calculated results are in good agreement with the experimental ones. Since the absolute values of the local magnetic moments of Mn, Cr ions in each doped compound do not change much with the increase of the doping level, ferromagnetic interactions between Mn ions and antiferromagnetic interactions between Cr ions have caused the total moments in the doped compound to first increase with the large Mn concentration and then decrease with the increase of the Cr concentration.

Cubic structure for compounds with $x \geqslant 0.3$ has been reported by Jonker [14]. Ideal cubic structures, in addition to the distorted ones discussed above, are adopted in the present work for the 0.5- and 0.75-doped compounds. The corresponding results are represented by solid dots on the dashed line in figure 2. It is found that there is no substantial difference between the results obtained with cubic structures and distorted ones. The moments for the 0.75-doped compounds with the two structures are equal to each other (see figure 2). The moment for the 0.5-doped compound with cubic structure is smaller than that of the compound with the distorted one, and is closer to the experimental data. Bents [12], using neutron diffraction, has found that FM interaction occurs for the compound with a level of Cr doping around 0.2, and that G-AFM and some FM interaction occurs for compounds with higher levels of Cr doping (such as $x = 0.75$). Comparing with these conclusions, it is found that the results obtained in the present calculation are essentially in agreement with the previous work by Jonker and Bents. The suggestion of FM structure made by Gilleo [13] does not seem to be reasonable.

3.3. Electronic structures

Figure 4(a) gives the total and partial DOS of $LaMn_{0.25}Cr_{0.75}O_3$ with the most stable FiM magnetic structure. The solid and dotted lines in the figure indicate the spin-up and spin-down bands, respectively. The distance between the two kinds of Cr ion, Cr_1 and Cr_2, and the Mn ions are 5.49 Å and 3.88 Å, respectively. There is no essential difference between the DOS of the two Cr ions. The bands located in the energy region from -2.5 to -7.5 eV are mainly contributed by O 2p states, and the bands in the range of 2.0 eV around the Fermi energy (E_F) are mainly contributed by the Mn and Cr 3d states. Comparing to the densities of states of $LaCrO_3$ in figure 1(b), it is found that Cr 3d bands shift to lower energies by about

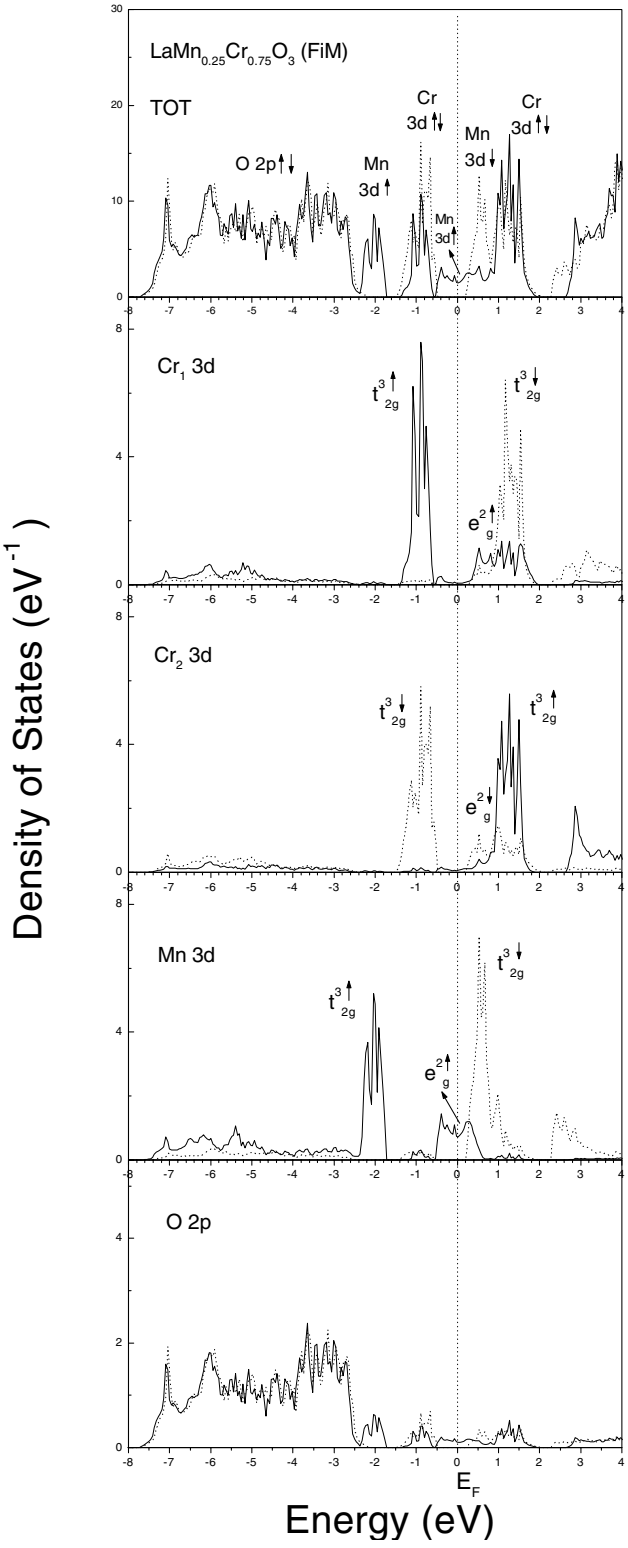

(a)

Figure 4. (a) The total and partial densities of states of $LaMn_{0.25}Cr_{0.75}O_3$ in the ferrimagnetic structure calculated to be the most stable. (b) The total and partial densities of states of $LaMn_{0.25}Cr_{0.75}O_3$ with ferromagnetic structure. The two kinds of Cr ion, Cr_1 and Cr_2, are further from and closer to the Mn ions, respectively. The solid and dotted lines indicate spin-up and spin-down bands, respectively.

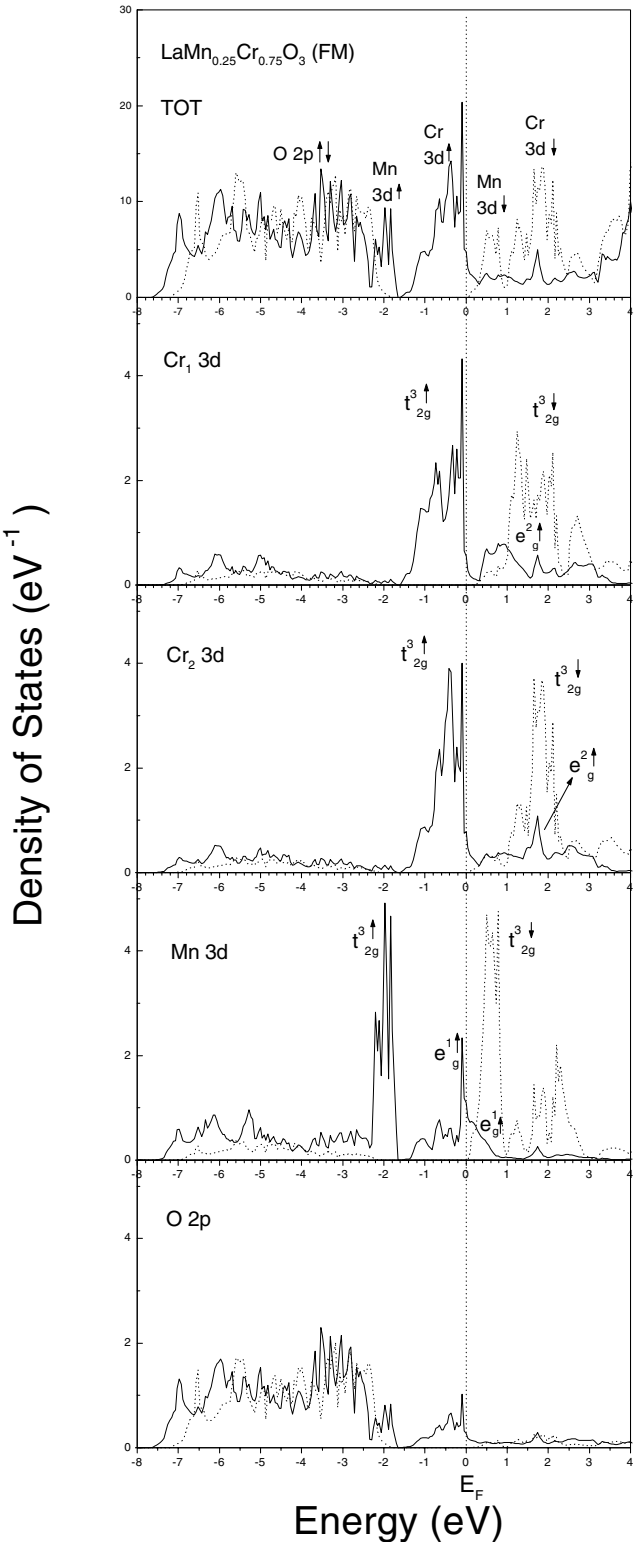

(b)

Figure 4. (Continued)

0.5 eV in the 0.75-doped compound, while the exchange splittings hardly change at all, which gives the result that the magnetic moments on Cr ions are approximately equal to each other in the two compounds. Moreover, the O 2p bands in figures 1(b) and 4(a) are also almost the same; and the spin polarizations in the two O 2p spectra are both very small. There are, however, large differences between the Mn 3d states in the 0.75-doped compound and those in $LaMnO_3$. The positions of the occupied and unoccupied t_{2g}^3 states do not differ much between the two compounds, while the occupied and unoccupied $e_g^1\uparrow$ states in $LaMnO_3$ both move obviously towards E_F, which leads to far more states existing across E_F in the 0.75-doped compound. Therefore, there exists a large gap between the occupied $t_{2g}^3\uparrow$ and $e_g^1\uparrow$ states and a similar situation also exists for the corresponding unoccupied states, which is due to the big splitting of the stronger crystal field in the 0.75-doped compound. Since the volume of the unit cell of $LaMn_{1-x}Cr_xO_3$ decreases with the increase of x, the crystal field becomes stronger with the increase of x. The band splitting induced by the crystal field increases accordingly. Although there are far more spin-up bands located near E_F, there are no spin-down bands across E_F, which gives rise to the so-called 'half-metallic' nature of the 0.75-doped compound. This half-metallic property has been found for several perovskites such as the doped systems $La_{1-x}Ca_xMnO_3$ [5], $La_{1-x}Ba_xMnO_3$ ($x > 0.33$) [22] and $LaMn_{0.5}Co_{0.5}O_3$ [8]. The CMR phenomena have been found for most of these compounds; thus, it has been suggested that the half-metallic nature may be responsible for the CMR properties. In the above-mentioned compounds, ferromagnetic structure usually exists together with the half-metallic bands, while half-metallic bands have been obtained in the present calculation for the 0.75-doped compound with both FM and FiM interaction (in several kinds of structure). In table 2, the total magnetic moments listed in the last row for the 0.75-doped compound are all integral [22], and, in fact, all correspond to half-metallic bands. The reason why integral moments always accompany half-metallic bands is still not very clear.

The stable magnetic interactions existing between Cr^{3+} and Cr^{3+} and between Mn^{3+} and Mn^{3+} ions in the doped compounds $LaMn_{1-x}Cr_xO_3$ can also be obtained by analysing the densities of states. Here, only the DOS of the 0.75-doped compound with FM structure and the most stable FiM structure are compared. Figure 4(b) gives the total and partial DOS of the 0.75-doped compound with the FM structure. The symbols for the ions correspond to those in figure 4(a). The solid and dotted lines also represent the spin-up and spin-down bands, respectively. It is found that there exists strong spin polarization between O 2p spin-up and spin-down bands in the FM states. Although there are no spin-down bands crossing E_F in figure 4(b), like in figure 4(a), there are far more occupied spin-up bands close to and across E_F. Since in the vicinity of E_F the occupied t_{2g}^3 states of Cr ions and the occupied and unoccupied e_g^1 states of Mn ions are all spin-up bands and there exist strong hybridizations between them, some of the Cr $t_{2g}^3\uparrow$ states cross E_F in figure 4(b) and smear out the big dip separating the t_{2g}^3 and e_g states of Cr ions at E_F shown in figure 4(a). This feature, which has caused E_F in figure 4(b) to lie at the spike below the small dip separating the t_{2g}^3 and e_g states of Cr ions, has made the state less stable than the magnetic phase in figure 4(a).

4. Conclusions

In conclusion, the magnetic and electronic properties of the Cr-doped manganese perovskites $LaMn_{1-x}Cr_xO_3$ ($x = 0.0, 0.25, 0.5, 0.75, 1.0$) have been investigated systematically by the tight-binding linear muffin-tin orbital method. Several different kinds of magnetic structure have been studied for doped compounds with intermediate doping levels. It is found that the ferromagnetic phase is not the stable state for those compounds, while a ferrimagnetic phase

of a certain type is the most stable. Due to the nearly cubic structure of the doped compounds, ferromagnetic interactions between Mn ions have been obtained. The interaction between Cr ions is antiferromagnetic; this has been analysed using DOS plots. The total magnetic moments varying with the level of Cr doping are in good agreement with the experimental ones, except for a small discrepancy for the 0.5-doped compound. Half-metallic bands, which are suggested to be related to the colossal magnetoresistance property of doped perovskites, have been found for the 0.75-doped compound with both ferromagnetic and ferrimagnetic phases of various types and the 0.5-doped compound with interlacing-type doping.

Acknowledgments

This work was supported by the National Natural Science Foundation of China (Grant No 19677202), National PAN-DENG project (Grant No 95-YU-41) and the Foundation of National High Performance Computing Centre, Shanghai, China.

References

[1] Von Helmolt R, Wecker J, Holzapfel B, Schultz L and Samwer K 1993 *Phys. Rev. Lett.* **71** 2331
[2] Jin S, Tiefel T H, McCormack M, Fastnacht R A, Ramesh R and Chen L H 1994 *Science* **264** 413
[3] Asamitsu A, Moritomo Y, Tomioka Y, Arima T and Tokura Y 1995 *Nature* **373** 407
[4] Satpathy S, Popović Z S and Vukajlović F R 1996 *Phys. Rev. Lett.* **76** 960
[5] Pickett W E and Singh D J 1996 *Phys. Rev.* B **53** 1146
[6] Millis A J 1998 *Nature* **392** 438
Booth C H, Bridges F, Kwei G H, Lawrence J M, Cornelius A L and Neumeier J J 1998 *Phys. Rev. Lett.* **80** 853
[7] Park J H, Cheong S W and Chen C T 1997 *Phys. Rev.* B **55** 11 072
[8] Yang Z, Ye L and Xie X 1999 *Phys. Rev.* B **59** 7051
[9] Phillipps M B, Sammes N M and Yamamoto O 1996 *J. Mater. Sci.* **31** 1689
[10] Goodenough J B, Wold A, Arnott R J and Menyuk N 1961 *Phys. Rev.* **124** 373
[11] Blasse G 1965 *J. Phys. Chem. Solids* **26** 1969
[12] Bents U H 1957 *Phys. Rev.* **106** 225
[13] Gilleo M A 1957 *Acta Crystallogr.* **10** 161
[14] Jonker G H 1956 *Physica* **22** 707
[15] Andersen O K 1975 *Phys. Rev.* B **12** 3060
Skriver H L 1984 *The LMTO Method* (Berlin: Springer)
Andersen O K and Jepsen O 1984 *Phys. Rev. Lett.* **53** 2571
[16] Hamada N, Sawada H and Terakura K 1995 *Spectroscopy of Mott Insulators and Correlation Metals* ed A Fujimori and Y Tokura (Berlin: Springer)
[17] Arima T, Tokura Y and Torrance J B 1993 *Phys. Rev.* B **48** 17 006
[18] Solovyev I and Hamada N 1996 *Phys. Rev.* B **53** 7158
Yang Z, Huang Z, Ye L and Xie X 1999 *Phys. Rev.* B **60** 15 674
[19] Koehler W C and Wollan E O 1957 *J. Phys. Chem. Solids* **2** 100
[20] Elemans J B A A, Van Laar B, Van der Veen K R and Loopstra B O 1971 *J. Solid State Chem.* **3** 238
[21] Goodenough J B 1955 *Phys. Rev.* **100** 564
[22] Youn S J and Min B I 1997 *Phys. Rev.* B **56** 12 046